

# Self-Propelled Carbohydrate-Sensitive Microtransporters with Built-In Boronic Acid Recognition for Isolating Sugars and Cells

Filiz Kuralay, Sirilak Sattayasamitsathit, Wei Gao, Aysegul Uygun, Adlai Katzenberg, and Joseph Wang\*

Department of Nanoengineering, University of California—San Diego, La Jolla, California 92093, United States

**S** Supporting Information

**ABSTRACT:** A new nanomotor-based target isolation strategy, based on a “built-in” recognition capability, is presented. The concept relies on a poly(3-aminophenylboronic acid) (PAPBA)/Ni/Pt microtube engine coupling the selective monosaccharide recognition of the boronic acid-based outer polymeric layer with the catalytic function of the inner platinum layer. The PAPBA-based micro-rocket is prepared by membrane-templated electropolymerization of 3-aminophenylboronic acid monomer. The resulting boronic acid-based microengine itself provides the target recognition without the need for additional external functionalization. “On-the-fly” binding and transport of yeast cells (containing sugar residues on their wall) and glucose are illustrated. The use of the recognition polymeric layer does not hinder the efficient propulsion of the microengine in aqueous and physiological media. Release of the captured yeast cells is triggered via a competitive sugar binding involving addition of fructose. No such capture and transport are observed in control experiments involving other cells or microengines. Selective isolation of monosaccharides is illustrated using polystyrene particles loaded with different sugars. Such self-propelled nanomachines with a built-in recognition capability hold considerable promise for diverse applications.

Locomotion of synthetic nano-/microscale objects through fluid environments is one of the most exciting and challenging areas of nanotechnology.<sup>1–5</sup> Self-propelled nano-/microscale machines hold great promise for performing diverse operations and important tasks, ranging from delivery of therapeutic payloads<sup>6</sup> to environmental remediation.<sup>7</sup> Chemically powered tubular microengines have been particularly attractive and powerful for diverse practical applications due to their efficient bubble-induced propulsion in relevant biological fluids and high ionic strength environments.<sup>8–11</sup> Such microengines are commonly prepared by thin-film rolled-up technology<sup>8</sup> or template membrane electrodeposition<sup>9</sup> to yield multilayer microtubes (~5–100 μm long, with tube openings of 1–10 μm) containing an inner catalytic platinum surface. Polymer/Pt microengines offer record-breaking speed of over 1000 body lengths/sec,<sup>12,13</sup> reflecting a large force and power essential to execute different tasks. The outer polymeric layer, commonly polyaniline (PANI) or poly(3,4-ethylenedioxythiophene) (PEDOT), has no active role besides supporting the metal catalyst deposition.

Functionalized microtube engines have been shown useful for the selective isolation of target biomolecules and cells from raw biological media by capturing and transporting them to a clean environment.<sup>10,11,14–16</sup> This attractive nanomachine isolation strategy commonly requires additional fabrication and immobilization steps for functionalizing the microengines with the corresponding bioreceptor, through sputtering of the outer microtube surface with a gold layer, followed by the self-assembly of a mixed alkanethiol monolayer and covalent coupling of the bioreceptor. Microengines functionalized with aptamers, antibody, lectin, or oligonucleotide have thus shown extremely useful as self-propelled microtransporters for cancer cells,<sup>10</sup> nucleic acid,<sup>11</sup> proteins,<sup>15</sup> or bacteria,<sup>16</sup> respectively.

This Communication describes a new nanomachine-based “capture-and-transport” strategy for isolating biological targets that does not require separate functionalization step with an additional receptor but exploits the built-in recognition properties of the outer polymeric layer itself. The new microtransporter separation concept relies on a poly(3-aminophenylboronic acid) (PAPBA)/Ni/Pt microtube engine (Figure 1), coupling the recognition of monosaccharides by the boronic acid-based outer polymeric layer with the catalytic function of the inner Pt layer for “on-the-fly” binding and

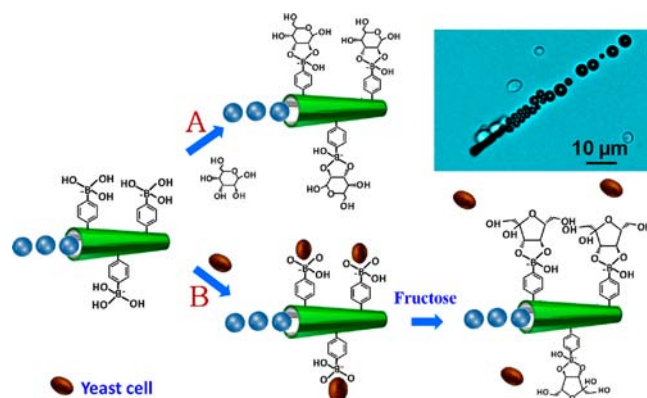


**Figure 1.** Microrocket with “built-in” boronic acid recognition of sugars and cells. Schematic representation of the poly(3-aminophenylboronic acid) (PAPBA)/Ni/Pt microrocket and its “on-the-fly” interaction with (A) glucose and (B) yeast cell, along with triggered (fructose-induced) release of the cell. Inset image shows a carbohydrate-sensitive microrocket transporting multiple yeast cells (W303 strain) (based on SI Video 1).

Received: June 21, 2012

Published: September 4, 2012

transport of target sugars. The complexation of monosaccharides with the boronic acid ligand is well established.<sup>17</sup> Different monosaccharide sensors based on this boronic acid complexation have been developed,<sup>18</sup> including electrochemical biosensors based on electropolymerized PAPBA.<sup>18f</sup> The ability of boronic acids to bind glucose has long been known<sup>18g,h</sup> and has been widely used for the sensing glucose in connection to the management of diabetes.<sup>19</sup>

Template electrodeposition of a PAPBA outer layer of the polymer/Ni/Pt microtube engine is used here for imparting the “built-in” monosaccharide recognition onto the moving microengine (Figure 1). The resulting carbohydrate-sensitive microengines have been shown useful for capturing and transporting glucose (Figure 1A) and for binding and releasing yeast cells containing sugar residues on their wall (Figure 1B). For example, the inset of Figure 1 illustrates the ability of the new PAPBA/Ni/Pt microengine to transport multiple yeast cells. Efficient bubble propulsion at a speed of  $80 \mu\text{m s}^{-1}$ , along with directional transport of the six cells, is observed from the corresponding video (SI Video 1). The similar size scale of the microengine and cells facilitates real-time visualization of the binding process. Notice the strong adherence of the cells to the fast moving microengine despite of its sharp maneuvers and trajectory changes. Apparently, the outer PAPBA layer, containing the recognition moieties, does not hinder the efficient bubble propulsion and high speed inherent to polymer/Pt bilayer microtube engines.<sup>12</sup> These and subsequent data also indicate that the electropolymerization process does not compromise the inherent sugar recognition properties of the monomer, as expected from early biosensor efforts.<sup>18f</sup>

An SEM image of the electrochemically prepared PAPBA/Pt microrockets, shown in SI Figure 1a, illustrates the conical microtubular structure of the resulting microengines. The resulting microrockets are  $\sim 10 \mu\text{m}$  long and have front inner and outer opening diameters of  $\sim 0.8$  and  $\sim 1.0 \mu\text{m}$ , respectively. Such shape is essential for generating the bubble thrust and reflects the micropores of the polycarbonate membrane template. Similar conical microtube engines have been reported using outer polymeric layers (e.g., PANI, PEDOT, or polypyrrole)<sup>12</sup> that do not possess a recognition ability. The intermediate Ni layer allows convenient magnetic control of the microrocket motion, as illustrated in SI Figure 1b and SI Video 2. This video illustrates an efficient magnetic guidance of the PAPBA/Ni/Pt microengine in human serum at a speed of  $40 \mu\text{m s}^{-1}$ , which is similar to that of other polymeric tubular microengines in physiological media containing 5%  $\text{H}_2\text{O}_2$  fuel,<sup>12</sup> indicating effective propulsion in physiological media.

Figure 2, along with the corresponding SI Video 3, illustrates the ability of the carbohydrate-sensitive microengine to approach (a), capture (b), transport (c), and release (d) a yeast cell. Such an on-the-fly capture process reflects the nearly instantaneous recognition of the cell-wall glucose residues by the boronic acid-based microengine. The microrocket speed is reduced from  $40$  to  $20 \mu\text{m s}^{-1}$  after capturing the yeast cell (in the presence of the 3%  $\text{H}_2\text{O}_2$  fuel and 1.5% NaCh). Such slower speed reflects the increased drag force associated with the larger and asymmetric motor/cell object.<sup>20</sup> Triggered unloading of the captured cell is also illustrated in Figure 2d (and SI Video 3) in connection to addition of 20 mM fructose, which has a stronger binding affinity for the boronic acid ligand.<sup>21</sup> Such competitive sugar binding thus leads to on-the-fly detachment of the captured yeast cell toward subsequent

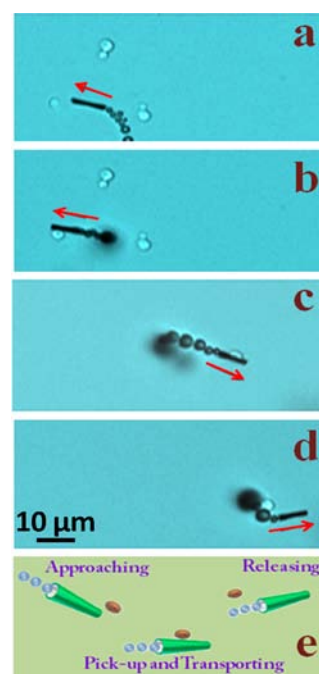


**Figure 2.** “Capture–transport–release” of yeast cells (based on SI Video 3): a PAPBA/Ni/Pt microrocket approaching (a), capturing (b), transporting (c), and releasing (d) the yeast cell. (e) Schematic representation of the capture–transport–release process. Conditions: 50 mM phosphate buffer (pH 8.5) containing 150 mM NaCl, 3%  $\text{H}_2\text{O}_2$ , and 1.5% sodium cholate; 20 mM fructose used in (d) for triggering the release of the cell.

reuse of the microengine, analogous to the release reported for single-cell electrode arrays.<sup>21</sup> Over the experimental time scale, a large fraction of the cells is expected to maintain its viability in the peroxide fuel medium. In general, the new boronic acid-based nanomotor strategy allows for isolation of different yeast cell populations (independent of their viability). The ability to isolate dead cells is also attractive for tracing the source of an outbreak. A wide range of peroxide-free nanomotors (water-driven, magnetically or ultrasound actuated) could be combined with PAPBA polymer, and hence be used to ensure full viability of the yeast cell targets.<sup>22</sup>

The specificity of the PAPBA/Ni/Pt microrocket to the yeast cell is illustrated in the control experiments of Figure 3. For example, no binding and transport are observed in Figure 3A in the presence of a 5-fold excess of the urinary pathogen *Staphylococcus aureus* ( $1 \mu\text{m}$  diameter) containing mannose in its cell wall. The PAPBA used here is known to have a substantially higher affinity to glucose than mannose.<sup>23</sup> As illustrated in the corresponding SI Video 4, the PAPBA/Ni/Pt microrocket is contacting but not capturing or transporting the round-shaped *S. aureus*. An additional control experiment involved yeast cells along with another polymer-based microrocket, PEDOT/Ni/Pt,<sup>12</sup> that does not possess a carbohydrate recognition ability (Figure 3B(a–c) and SI Video 5). As expected, the direct deliberate contact of the yeast cell with the PEDOT/Ni/Pt microrocket does not lead to the capture and transport processes observed with the carbohydrate-sensitive PAPBA-based microengine.

The selectivity and scope of the new microengine-target isolation protocol have been examined also by incubating different saccharides with  $2 \mu\text{m}$  microsphere tags for the direct visualization of the motor–saccharide interaction. As expected,

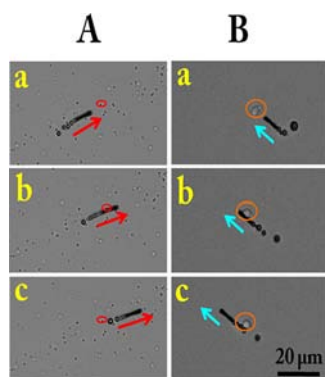


**Figure 3.** Selectivity of the PAPBA/Ni/Pt microrockets: (A) A PAPBA/Ni/Pt microrocket approaching (a), contacting (b), and moving without capturing (c) a *S. aureus* cell. (B) A PEDOT/Ni/Pt microrocket approaching (a), contacting (b), and continually moving without carrying (c) the yeast cell. Conditions as in Figure 2. (A) and (B) are based on SI Videos 4 and 5, respectively.

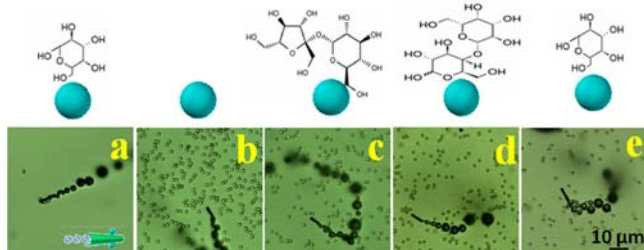


**Figure 4.** Selectivity and scope of the motor isolation protocol. Interactions of the PABPA/Ni/Pt microrocket with 7 mM glucose-incubated PS (a), bare PS (b), 70 mM sucrose-incubated PS (c), 70 mM lactose-incubated PS (d), and PANI/Ni/Pt microrocket with 7 mM glucose-incubated PS (e). Conditions as in Figure 2. Images a–e are based on SI Video 7.

and clearly illustrated in Figure 4 and the corresponding SI Videos 6 and 7, the moving PAPBA-based microengine selectively interacts with the glucose monosaccharide (7 mM) (a), but not with a 10-fold excess of the sucrose (c) or lactose (d) disaccharides. Similarly, no capture and transport processes are observed using the PAPBA/Ni/Pt microrocket in the presence of a large excess of unmodified microspheres (b) or using the glucose-loaded sphere along with a “control” PANI/Ni/Pt microrocket (e). As illustrated in SI Figure 2 and SI Video 6, the initial speed of the microrocket is reduced from 20 to 16  $\mu\text{m s}^{-1}$  after capturing a glucose-loaded sphere.

UV–vis spectroscopy, based on a dye–boronic acid affinity reaction, was also used for monitoring and verifying the chemical interaction between the PAPBA/Ni/Pt microrockets and glucose molecules (SI Figure 3). Alizarin Red S (ARS), which is commonly used for probing the binding of boronic acid with carbohydrates,<sup>24</sup> displays a distinct changes in the absorbance intensity and maximum wavelength in response to binding with boronic acid and subsequent displacement of the dye from the complex. As expected and illustrated in SI Figure 3, the absorption peak of ARS (a) shifted to shorter wavelength after adding the boronic acid-functionalized microrockets into the dye solution (b). Additions of 5 and 10 mM glucose into the dye/boronic acid complex solution resulted in successive diminutions of the complex peak (c and d, respectively), indicating the displacement of ARS by glucose.<sup>24</sup>

In conclusion, we have described a new nanomachine-based capture and transport strategy exploiting the “built-in” recognition properties of the outer polymeric layer itself for isolating target sugars and cells. The new concept has been illustrated in connection to PAPBA-based nanomachines whose outer polymeric layer provides the specific monosaccharide recognition. The polymer layer thus acts as the receptor recognizing the target biomolecule, eliminating the need for additional receptor functionalization steps. These template-prepared carbohydrate-sensitive microengines offer very attractive capabilities for autonomous loading, directional transport, and triggered unloading (“catch and release”) of monosaccharides and yeast cells. Controlled release of the captured cells toward subsequent reuse has been accomplished by the addition of fructose. This new carbohydrate-sensitive nanomachine concept can be expanded further toward a glucose-responsive controlled insulin delivery.<sup>25</sup> While the concept of nanomachines with a built-in recognition has been illustrated here for isolating monosaccharides and cells it could be readily extended to the capture and transport of other important target molecules in connection to outer polymeric layers with different recognition capabilities.

## ■ ASSOCIATED CONTENT

### 📄 Supporting Information

Microrocket preparation, related protocols, instrumentation, reagents, additional data, and videos. This material is available free of charge via the Internet at <http://pubs.acs.org>.

## ■ AUTHOR INFORMATION

### Corresponding Author

josephwang@ucsd.edu

### Notes

The authors declare no competing financial interest.

## ■ ACKNOWLEDGMENTS

This work was supported by the U.S. Defense Threat Reduction Agency. S.S.’s salary was supported by a grant from the Department of Energy (DOE BES DE-SC0004937). W.G. is a Howard Hughes Medical Institute International Student Research fellow. The authors thank Natalie A. Cookson for providing the yeast cells.

## ■ REFERENCES

- (1) (a) Paxton, W. F.; Kistler, K. C.; Olmeda, C. C.; Sen, A.; Angelo, S. K.; St.; Cao, Y.; Mallouk, T. E.; Lammert, P. E.; Crespi, V. H. *J. Am. Chem. Soc.* **2004**, *126*, 13424. (b) Fournier-Bidoz, S.; Arsenault, A. C.; Manners, I.; Ozin, G. A. *Chem. Commun.* **2005**, *41*, 441. (c) Ozin, G. A.; Manners, I.; Fournier-Bidoz, S.; Arsenault, A. *Adv. Mater.* **2005**, *17*, 3011.
- (2) Wang, J. *ACS Nano* **2009**, *3*, 4.
- (3) Mallouk, T. E.; Sen, A. *Sci. Am.* **2009**, *300*, 72.
- (4) Pumera, M. *Nanoscale* **2010**, *2*, 1643.
- (5) (a) Loget, G.; Kuhn, A. *J. Am. Chem. Soc.* **2010**, *132*, 15918. (b) Zhang, L.; Abbott, J. J.; Dong, L. X.; Kratochvil, B. E.; Bell, D.; Nelson, B. J. *Appl. Phys. Lett.* **2009**, *94*, 064107. (c) Pavlick, R. A.; Sengupta, S.; McFadden, T.; Zhang, H.; Sen, A. *Angew. Chem., Int. Ed.* **2011**, *50*, 9374.
- (6) Kagan, D.; Laocharoensuk, R.; Zimmerman, M.; Clawson, C.; Balasubramanian, S.; Kang, D.; Bishop, D.; Sattayasamitsathit, S.; Zhang, L.; Wang, J. *Small* **2010**, *6*, 2741.
- (7) Guix, M.; Orozco, J.; Garcia, M.; Gao, W.; Sattayasamitsathit, S.; Merkoci, A.; Escarpa, A.; Wang, J. *ACS Nano* **2012**, *6*, 4445.

(8) (a) Mei, Y. F.; Huang, G. S.; Solovev, A. A.; Bermúdez Ureña, E.; Mönch, I.; Ding, F.; Reindl, T.; Fu, R. K. Y.; Chu, P. K.; Schmidt, O. G. *Adv. Mater.* **2008**, *20*, 4085. (b) Mei, Y. F.; Solovev, A. A.; Sanchez, S.; Schmidt, O. G. *Chem. Soc. Rev.* **2011**, *40*, 2109.

(9) (a) Gao, W.; Sattayasamitsathit, S.; Orozco, J.; Wang, J. *J. Am. Chem. Soc.* **2011**, *133*, 11862. (b) Gao, W.; Uygun, A.; Wang, J. *J. Am. Chem. Soc.* **2012**, *134*, 897.

(10) Balasubramanian, S.; Kagan, D.; Hu, C. M.; Campuzano, S.; Lobo-Castañon, M. J.; Lim, N.; Kang, D. Y.; Zimmerman, M.; Zhang, L.; Wang, J. *Angew. Chem., Int. Ed.* **2011**, *50*, 4161.

(11) Kagan, D.; Campuzano, S.; Salasubramanian, S.; Kuralay, F.; Flechsig, G. U.; Wang, J. *Nano Lett.* **2011**, *11*, 2083.

(12) Gao, W.; Sattayasamitsathit, S.; Uygun, A.; Pei, A.; Ponedal, A.; Wang, J. *Nanoscale* **2012**, *4*, 2447.

(13) Gao, W.; Sattayasamitsathit, S.; Wang, J. *Chem. Rec.* **2012**, *12*, 224.

(14) Wang, J. *Lab Chip* **2012**, *12*, 1944.

(15) Orozco, J.; Campuzano, S.; Kagan, D.; Zhou, M.; Gao, W.; Wang, J. *Anal. Chem.* **2011**, *83*, 7962.

(16) Campuzano, S.; Orozco, J.; Kagan, D.; Guix, M.; Gao, W.; Sattayasamitsathit, S.; Claussen, S. C.; Merkoci, A.; Wang, J. *Nano Lett.* **2012**, *12*, 396.

(17) (a) James, T. D.; Phillips, M. D.; Shinkai, S. *Boronic Acids in Saccharide Recognition*; RSC Publishing: Dorchester, UK, 2006. (b) Wang, W.; Gao, X. M.; Wang, B. H. *Curr. Org. Chem.* **2002**, *14*, 1285.

(18) (a) James, T. D.; Sandanayake, K. R. A. S.; Shinkai, S. *Angew. Chem., Int. Ed.* **1996**, *35*, 1910. (b) Kikuchi, A.; Suzuki, K.; Okabayashi, O.; Hoshino, H.; Kataoka, K.; Sakurai, Y.; Okano, T. *Anal. Chem.* **1996**, *68*, 823. (c) Pickup, J. C.; Hussain, F.; Evans, N. D.; Rolinski, O. J.; Birch, D. J. S. *Biosens. Bioelectron.* **2005**, *20*, 2555. (d) Takahashi, D.; Hirono, S.; Hayashi, C.; Igarashi, M.; Nishimura, Y.; Toshima, K. *Angew. Chem., Int. Ed.* **2010**, *49*, 10096. (e) Abad, J. M.; Velez, M.; Santamaria, C.; Guisan, J. M.; Matheus, P. R.; Vazquez, L.; Gazaryan, I.; Gorton, L.; Gibson, T.; Fernandez, V. M. *J. Am. Chem. Soc.* **2002**, *124*, 12845. (f) Aytac, S.; Kuralay, F.; Boyaci, I. H.; Unaleroglu, C. *Sens. Actuators B: Chem.* **2011**, *160*, 405. (g) Lorand, J. P.; Edwards, J. O. *J. Org. Chem.* **1959**, *24*, 769. (h) Tsukagoshi, K.; Shinkai, S. *J. Org. Chem.* **1991**, *56*, 4089.

(19) (a) Francesconi, K. A.; Pannier, F. *Clin. Chem.* **2004**, *50*, 2353. (b) Fang, H.; Kaur, G.; Wang, B. *J. Fluoresc.* **2004**, *14*, 481. (c) Park, S.; Boo, H.; Dong Chung, T. *Anal. Chim. Acta* **2006**, *556*, 46. (d) Kabilan, S.; Marshall, A. J.; Sartain, F. K.; Lee, M. C.; Hussain, A.; Yang, X.; Blyth, J.; Karangu, N.; James, K.; Zeng, J.; Smith, D.; Domschke, A.; Lowe, C. R. *Biosens. Bioelectron.* **2005**, *20*, 1602.

(20) Zhao, G.; Pumera, M. *Phys. Chem. Chem. Phys.* **2012**, *14*, 6456.

(21) (a) Polsky, R.; Harper, J. C.; Wheeler, D. R.; Arango, D. C.; Brozik, S. M. *Angew. Chem., Int. Ed.* **2008**, *47*, 2631. (b) Ma, Y.; Yang, X. *J. Electroanal. Chem.* **2005**, *580*, 348. (c) Torun, Ö.; Dudak, F. C.; Baş, D.; Tamer, U.; Boyaci, I. H. *Sens. Actuators B: Chem.* **2009**, *140*, 597.

(22) (a) Kagan, D.; Benchimol, M. J.; Claussen, J. C.; Chuluun-Erdene, E.; Esener, S.; Wang, J. *Angew. Chem., Int. Ed.* **2012**, *51*, 7637. (b) Gao, W.; Pei, A.; Wang, J. *ACS Nano* **2012**, *6*, DOI: 10.1021/nm303309z. (c) Gao, W.; Sattayasamitsathit, S.; Manesh, K. M.; Weihs, D.; Wang, J. *J. Am. Chem. Soc.* **2010**, *132*, 14403. (d) Wang, J.; Gao, W. *ACS Nano* **2012**, *6*, 5745.

(23) (a) Sun, X.-Y.; Liu, B.; Jiang, Y.-B. *Anal. Chim. Acta* **2004**, *515*, 285. (b) Li, S.; Davis, E. N.; Anderson, J.; Lin, Q.; Wang, Q. *Biomacromolecules* **2009**, *10*, 113.

(24) (a) Springsteen, G.; Wang, B. *Chem. Commun.* **2001**, *17*, 1608. (b) Cannizzo, C.; Amigoni-Gerbier, S.; Larpent, C. *Polymer* **2005**, *46*, 1269. (c) Springsteen, G.; Wang, B. *Tetrahedron* **2002**, *58*, 5291. (d) Lee, K.; Asher, S. A. *J. Am. Chem. Soc.* **2000**, *122*, 9534.

(25) Zhao, Y.; Trewyn, B. G.; Slowing, I. I.; Lin, V. S. Y. *J. Am. Chem. Soc.* **2009**, *131*, 8398.